

# We are IntechOpen, the world's leading publisher of Open Access books Built by scientists, for scientists

4,400

Open access books available

117,000

International authors and editors

130M

Downloads

Our authors are among the

154

Countries delivered to

TOP 1%

most cited scientists

12.2%

Contributors from top 500 universities



WEB OF SCIENCE™

Selection of our books indexed in the Book Citation Index  
in Web of Science™ Core Collection (BKCI)

Interested in publishing with us?  
Contact [book.department@intechopen.com](mailto:book.department@intechopen.com)

Numbers displayed above are based on latest data collected.  
For more information visit [www.intechopen.com](http://www.intechopen.com)



# The use of Switched Reluctance Generator in Wind Energy Applications

Eleonora Darie\*, Costin Cepișcă\*\* and Emanuel Darie\*\*\*

*\*Technical University of Civil Engineering Bucharest, Electrotechnical Department*

*\*\* University Polytechnic of Bucharest, Electrotechnical Department*

*\*\*\*Police Academy Bucharest, Engineering Department*

*Romania*

## 1. Introduction

Climate change is a contemporary issue. World are concerned about protecting the environment. Energy savings are a main strategy to get good results in the efforts to preserve the planet. Therefore, is required to develop and use new technologies. Wind power is a recent renewable primary energy source that must be considered in the future global energy. Wind power is one of the renewable energy power sources what help in reducing the carbon dioxide from the atmosphere. Various schemes for generating electricity from the wind have been proposed (Rim & Krishan, 1994). Wind power requires some special electric generator to work under continuously variable speed. In this context, the Switched Reluctance Generator (SRG) is investigated for to maximize wind power efficiency. This machine is robust, easy to construct and to maintain. In many aspects this kind of machine, now available, works better than others like the asynchronous machine. The absence of permanent magnets in the stator and windings in the rotor; low manufacturing costs; low maintenance; robustness; reliability; high efficiency; increased power density are some advantages of SRG side by side with a large range of operational speed. Despite they are somewhat noisy and its control is essentially non-linear the SRG was largely benefited with the recent advances on power electronics and micro processing. Torque, current and voltage ripples are inherent to the SRG, but the modern power electronic minimized these disadvantages. The principle of operation of this machine is known since the beginning of the electrical machines development. Soon the driving of these machines proved to be somewhat complex (Gail & Hansen, 2006). The advances on power electronics and micro processing in the last decade renewed the expectancies. In fact, modern power electronic converters associated with micro processed control hardware have brought competitiveness to SRG driven systems, allowing their efficient and reliable use. The SRG has shown great developing potential and study value in the area of wind power generation (Torrey, 2002). The SRG is a synchronous generator with a doubly salient construction, with salient poles on both the stator and the rotor. Excitation of the magnetic field is provided by the stator current in the same way as it is provided for the induction generator. The SRG is considered inferior to the Permanent Magnet Synchronous Generator

(PMSG) because of its lower power density (Darie & et al., 2007). The SRG requires a full-scale power converter in order to operate as a grid-connected generator. Moreover, the SRG has a lower efficiency than a PMSG and a lower power factor than asynchronous generators (Hansen, 2001). Through these advantages have already been confirming, some aspects of these machines must be mentioning here: there is a strong magnetic discontinuity providing current, voltage and torque ripples that should be properly controlling. The power electronics requirements to control a SRG are sometimes quoting as disadvantages of this kind of machine. Furthermore, they are a little noisy. Due to its advantages, SRG are considering as a special generator for wind power (Pan Zai-Ping et al. 2003). The switched reluctance machine SRM is an unsuccessful old idea now renewed by recent power electronics and microprocessors developments. It is a doubly salient pole and works as a motor or as a generator depending on the firing angles (Tadashi, 2001).

## 2. Linear mathematical model of SRG

Figure 1 shows the variation of inductance with rotor position for one phase winding, idealized in that magnetic saturation and the rounding effect of the fringing fields are neglected (Miller et al., 1990). According to the above suppositions, the mathematical model of SRG is ideal and linear (Gail & Hansen, 2006).

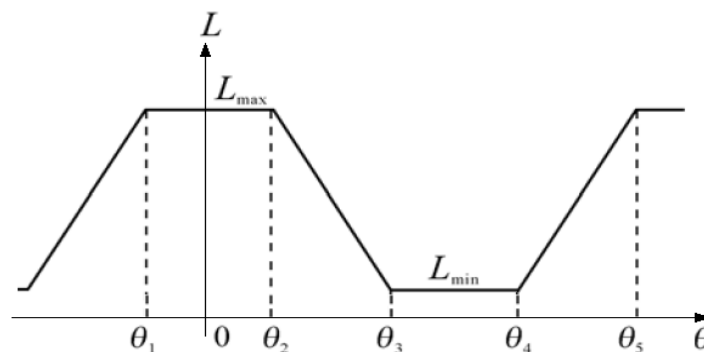


Fig. 1. The relationship between inductance and the position of the rotor in ideal and linear mathematical model.

The iron cores of the stator and the rotor in SRG are all protruding poles. The distribution of magnetic field is different when the relative position between rotor pole and the electrified phase on the stator is different. So the winding inductance  $L$  will change along with the change of the relative position between rotor pole and stator pole. When the rotor is turning, the inductance of windings will change from the maximum  $L_{max}$  to the minimum  $L_{min}$  periodically (Pan Zai-Ping et al. 2003). The inductance reaches maximum when the axes of rotor and stator pole are in the same position and reaches minimum when the axis of the rotor pole and the center of the stator pole are in the same position. The relationship between inductance  $L(\theta)$  and the position of the rotor  $\theta$  can be shown through the following function (Chen et al., 2001):

$$L(\theta) = \begin{cases} L_{\max} - K(\theta_1 - \theta) & \theta_{on} \leq \theta < \theta_2 \\ L_{\max} & \theta_1 \leq \theta < \theta_2 \\ L_{\max} - K(\theta - \theta_2) & \theta_2 \leq \theta < \theta_3 \\ L_{\min} & \theta_3 \leq \theta < \theta_4 \\ L_{\max} - K(\theta - \theta_4) & \theta_4 \leq \theta < \theta_5 \end{cases} \quad (1)$$

Among the functions,  $\theta_{on}$  is the turn-on angle  $K = (L_{\max} - L_{\min}) / (\theta_3 - \theta_2)$ .

Suppose  $\theta_{on} \leq \theta_1, \theta_2 \leq \theta_{off} \leq \theta_3, \theta_4 \leq (2\theta_{off} - \theta_{on}) \leq \theta_5$ .

The change of phase current can be divided into six phases: (1) Starting phase:  $\theta_{on} \leq \theta \leq \theta_1$ ; (2) Rising linearly phase:  $\theta_1 \leq \theta \leq \theta_2$ ; (3) Rising continuously phase:  $\theta_2 \leq \theta \leq \theta_{off}$ ; (4) Generating phase:  $\theta_{off} \leq \theta \leq \theta_3$ ; (5) Falling linearly phase:  $\theta_3 \leq \theta \leq \theta_4$ ; (6) Falling continuously phase:  $\theta_4 \leq \theta \leq \theta_5$ .

The six phases of the phase current's change can be shown by uniform function below (Pan Zai-Ping et al. 2003):

$$i(\theta) = \begin{cases} \frac{u}{\omega L(\theta)}(\theta - \theta_{on}) & \theta_{on} \leq \theta \leq \theta_{off} \\ \frac{u}{\omega L(\theta)}(2\theta_{off} - \theta_{on} - \theta) & \theta_{off} \leq \theta < (2\theta_{off} - \theta_{on}) \end{cases} \quad (2)$$

The analytic function of the flux ( $\psi(\theta) = L(\theta)i(\theta)$ ) can be obtained as:

$$\psi(\theta) = \begin{cases} \frac{u}{\omega}(\theta - \theta_{on}) & \theta_{on} \leq \theta \leq \theta_{off} \\ \frac{u}{\omega}(2\theta_{off} - \theta_{on} - \theta) & \theta_{off} \leq \theta < (2\theta_{off} - \theta_{on}) \end{cases} \quad (3)$$

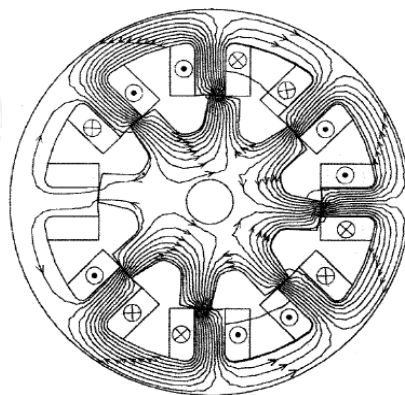


Fig. 2. Flux plots when one of eight coils is unexcited.

Figure 2 shows the flux distribution when one of eight coils is unexcited. Under this condition, unbalanced lateral forces will produce, and this may lead to mechanical failure.

### 3. Analysis of energy

Neglecting the resistance loss, medium loss and mechanical loss, the following equation can be obtained:

$$\pm ui = Li \frac{di}{dt} + i^2 \frac{dL}{d\theta} \omega \quad (4)$$

For generating state, the input electrical energy and the output mechanical energy are all negative, which means mechanical energy is converted into electrical energy. Based on the linear mathematical models of phase current and flux established above, the change of magnetic field energy state can be drawn as shown in Figure 3.

The turn-on angle in Figure 3,  $\theta_{on} = \theta_1$  and the process of the magnetic field energy's variation in one period can be seen very clearly in the figure. The change of magnetic field energy in one period is zero and magnetic field just act as medium in the whole energy changing process. Thereby, the variation of mechanical energy and electrical energy in one period can be known through reviewing the variation of the magnetic field energy (Pan Zai-Ping et al. 2003).

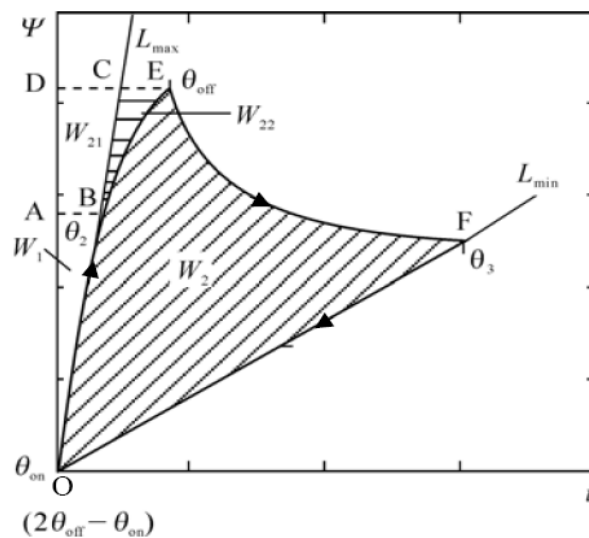


Fig. 3. The change of magnetic field energy state.

As shown in Figure 3, electrical source electrifies from  $\theta_{on}$  to  $\theta_{off}$  in one period. From  $\theta_1$  to  $\theta_2$ , the whole input electrical energy from the source is converted into magnetic field energy  $W_1$  and stored in the magnetic field because  $dL/d\theta=0$  and its magnitude is equal to the area of OAB. From  $\theta_2$  to  $\theta_{off}$  the input electrical energy from the source  $W_{21}$  (the area of ABCD) and the mechanical energy  $W_{22}$  (the area of BCE) are converted into magnetic field energy, because  $dL/d\theta < 0$ . The phase current is attenuates to zero at:  $2\theta_{off} - \theta_{on}$  (Pan Zai-Ping et al. 2003).

In this process, from  $\theta_{off}$  to  $\theta_3$ ,  $dL/d\theta < 0$ , the mechanical energy is converted into magnetic field energy constantly. From  $\theta_3$  to  $2\theta_{off} - \theta_{on}$   $dL/d\theta = 0$ , there is no input of mechanical energy and all the magnetic field energy is converted into electrical energy for output, which is shown as  $W_2$  (the area of OBEFO) in Figure 3. The whole magnetic field energy converted

from mechanical energy in one period is:  $W_2+W_{22}$ , which is the effective electromagnetic energy (the area of OBCEFO). Enhancing the generating ability of the generator should start with enhancing the effective electromagnetic energy (Pan Zai-Ping et al. 2003).

The way for enhancing the effective electromagnetic energy, should be considered in two parts below: (1) With increasing the maximum inductance or decreasing the minimum inductance, the area of  $W_2+W_{22}$ , will be increased; (2) The main way to improve the generation ability is to adjust the turn-on and turn-off angle (Pan Zai-Ping et al. 2003).

#### 4. Mode of operation by SRG

According to the existing research, most of the small wind turbine generators use a permanent magnet machine which has a cogging torque ( $T_c$ ) due to the existence of a permanent magnet. Cogging torque is the force that created between permanent magnet (PM) and a metal due to the PM characteristics (Lobato & Pires, 2003).

##### 4.1 SRG Characteristics

In electrical drives with variable reluctance (Figure 4), the torque is function of the regular position of the rotor due the double salient poles. The operation of the machine as a generator is obtained by energizing the windings of the stator when the salient poles of the rotor are away from their aligned position due to the rotating motion of the prime mover.

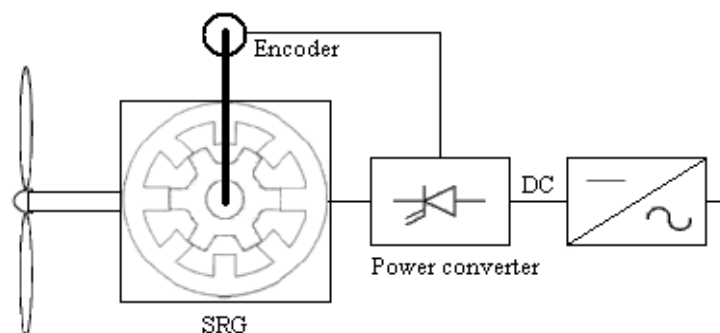


Fig. 4. The Switched reluctance generator in the wind turbine.

The SRG is characterized by the mode of controlling its phase current. For this problem the power electronic converter is used, which functions in a way that the phase currents of the machine are imposed for certain positions of the rotor. In this work is used the standard topology of the converter usually applied in SRM drives, given that it provides a greater flexibility regarding its control and better fault tolerance. The control system of this converter must regulate the magnitude and even the wave shapes of the phase currents to fulfill the requirements of torque and output power available and to ensure safe operation of the generator. This implies that the electronic switches associated with the controller are fully controlled devices. The topology (Figure 5) used power transistors (IGBT or MOSFET) that work as electronic switches. The capacitor shown in this topology prevents fluctuations in the voltage  $V_s$ . If losses are neglected the output energy over each stroke exceeds the excitation by the mechanical energy supplied (Hansen, 2001). One considers that there is no magnetic saturation and each phase is magnetically independent from others.

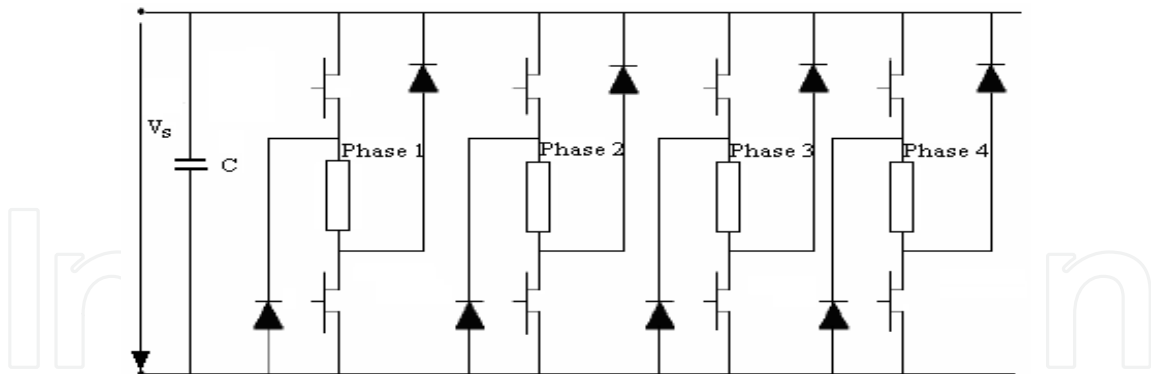


Fig. 5. The Switched reluctance generator in the wind turbine.

The SRM is characterized by the mode of controlling its phase current. For this problem the power electronic converter is used, which functions in a way that the phase currents of the machine are imposed for certain positions of the rotor. In this work is used the standard topology of the converter usually applied in SRM drives, given that it provides a greater flexibility regarding its control and better fault tolerance.

If losses are neglected the output energy over each stroke exceeds the excitation by the mechanical energy supplied (Hansen, 2001). On considers that there is no magnetic saturation and each phase is magnetically independent from others.

In these terms, the expression of the instantaneous power,  $p$ , available in the SRG is expressed as follow:

$$p(\theta, i_1, i_2, \dots, i_n) = \frac{1}{2} \left[ \sum_{j=1}^n \frac{dL_j(\theta)}{d\theta} i_j^2 \right] \omega, \quad (5)$$

where:  $n$  - the number of phases;  $j$  - the phase number;  $\theta$  - rotor position;  $\omega$  - rotor speed;  $i_j$  - the current phase,  $L_j(\theta)$  - the inductance of phase  $j$  as the function of  $\theta$ .

The average of power available  $P$ , resulting from the operation of the machine as a generator, is (with excluding the losses) equal to the mechanical power. The values can be obtained from the expression of the average value of the torque  $T_m$  using (6) and (7):

$$P = T_m \omega, \quad (6)$$

$$T_m = \frac{N_r}{2\pi} \int_0^{2\pi/N_r} \left[ \sum_{j=1}^n \frac{1}{2} \frac{dL_j}{d\theta} i_j^2 \right] d\theta, \quad (7)$$

where:  $N_r$  is the number or rotor poles.

The above equations enable us to infer that the obtained power is approximately constant and it reaches a maximum when the dwell angle is located, in the descending section of the phase inductance profile, which corresponds to the highest average torque (Akhmatov et al., 2001), (Henao & Bassily, 1997).

For this type of machines the torque ripple appears mainly in the commutation zones related with the sequential process of establishing and removing the phase currents.

The imposition of phase current waveform using the current control with an adjusted hysteresis band and a sufficient input voltage, allow the torque ripple reduction. In this way the ripple can be minimized, thus controlling the phase's currents commutation precisely phased relative to the rotor position. For that effect, the current control is done is done using the trapezoidal phase reference torque model (Grauers, 1997), two adjacent phases can be supplied at the same time to ensure the continuity in the generated torque. The SRM is capable of operating continuously as a generator by keeping the dwell angle so that the bulk of the winding conduction period comes after the aligned position, when  $\frac{dL_j}{d\theta} < 0$ . The waveforms of the phases reference current  $i_j^*$ , results from the desired torque  $T^*$  and is calculated by the following equation (Darie & et al., 2009, 2008):

$$i_j^* = \sqrt{\frac{2T_j^*}{\frac{dL_j(\theta)}{d\theta}}} \quad (8)$$

and are themselves the reference signals to be treated using the feedback pulse with modulation (PWM) with adjusted hysteresis band.

#### 4.2 SRG – The Current Control

The block diagram from the Figure 6, indicates the current control with the torque reference applied to the 8/6 SRG.

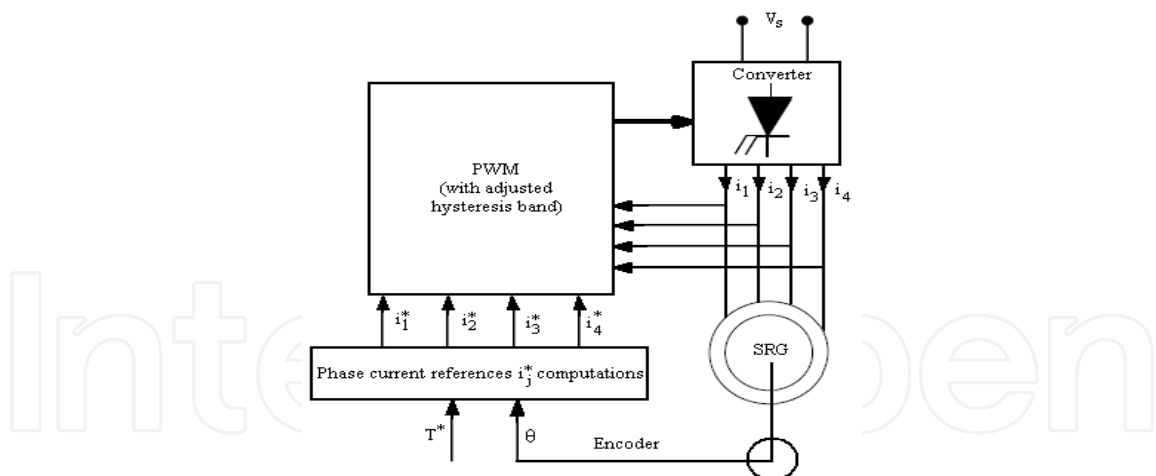


Fig. 6. The current control with the torque reference applied to 8/6 SRG.

The waveforms of the reference currents,  $i_1^*$ ,  $i_2^*$ ,  $i_3^*$  and  $i_4^*$ , are calculated using the trapezoidal model torque associated to each phase,  $T_1^*$ ,  $T_2^*$ ,  $T_3^*$  and  $T_4^*$ .



### 4.3 SRG – Simulations

On used for simulations an 8/6 SRG, with  $P_n=2.4$  kW, 4 phase. In these simulation examples of the SRG operation, the converter voltage used was  $V_s=800$  V, which allow reduced torque ripple and the rotor speed is 1000 rpm.

Figure 7 shows the phase current resulting from the trapezoidal phase torque.

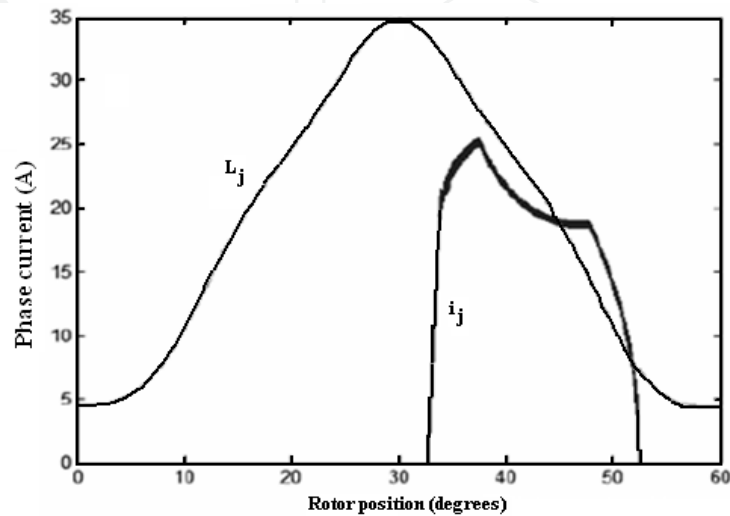


Fig. 7. Phase Current.

In Figure 8, is indicated the total instantaneous torque for 8/6 SRG.

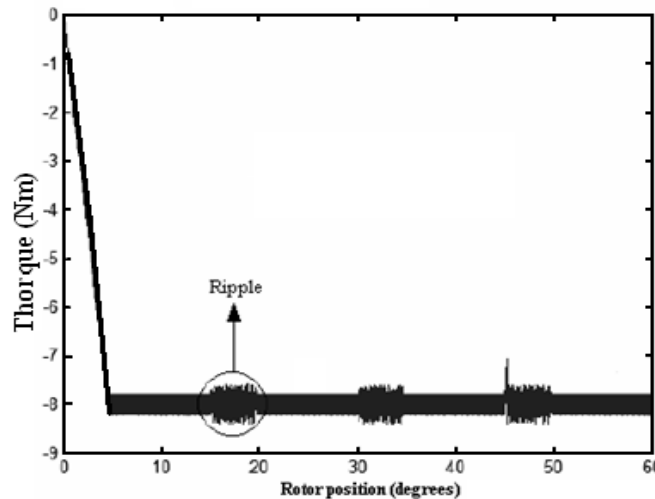


Fig. 8. Total Torque.

In order to achieve higher performance in SRG operation and higher efficiency in the conversion on includes optimal dwell angle control to further reduce the torque ripple.

## 5. Energy Conversion

In a SRG mechanical power achieved from a prime mover through a shaft is converted into electrical power. When a pole of the rotor is aligned with the excited pole of the stator, there is a state of stable equilibrium. Thus, in the SRG there is a natural tendency to align the rotor and the stator active poles in order to maximize the inductance of the phase. When an external mechanical agent forces the rotor to leave the stable equilibrium position, the electromagnetic torque produced results in a back electromotive force that increases the applied voltage. In this way the machine generates electrical power.

The electrical equation for a phase of the SRG is:

$$U = Ri + L \frac{di}{dt} + E \quad (9)$$

Where the back electromotive force EMF is given by equation (10):

$$E = i\omega \frac{\partial L}{\partial \theta}, \quad (10)$$

where:

$$\omega = \frac{d\theta}{dt}.$$

The stator is fed in DC. As  $\omega$  and  $i$  are both positive, the sign of  $E$  is the same as that of  $\partial L/\partial \theta$ . From the equation (2), it can be seen that when  $(\partial L/\partial \theta) > 0$ . In this case, electrical power is converted to mechanical power and the machine works as a motor. But when  $(\partial L/\partial \theta) < 0$  the back electromotive force is negative and it increases the current converting mechanical power into electrical power.

In (9) and (10),  $U$  - applied voltage;  $i$  - phase current;  $R$  - phase resistance,  $L$  - phase inductance;  $E$  - back electromotive force;  $\omega$  - rotor angular speed;  $\theta$  - rotor angular position;  $t$  - time.

The dynamic mechanical equation for the SRG is given by (11). It is to be noted that the electromagnetic torque  $C_{emag}$  comes as a negative quantity, acting against the rotor mechanical speed.

$$C_m + C_{emag} - J \frac{d\omega}{dt} - D\omega = 0, \quad (11)$$

where:  $C_m$  - applied mechanical torque,  $J$  - moment of inertia;  $D$  - coefficient of friction.

The co-energy of a phase of this machine is given by follow:

$$W^{co} = \int_0^i \lambda di \quad (12)$$

The corresponding electromagnetic torque for a phase SRG is given by:

$$C_{emag} = \frac{\partial W_a^{co}}{\partial \theta} + \frac{\partial W_b^{co}}{\partial \theta} + \frac{\partial W_c^{co}}{\partial \theta}. \quad (13)$$

The mathematical model of 6x4 SRG is shown below:

$$\begin{bmatrix} U_a \\ U_b \\ U_c \\ C_m \\ 0 \end{bmatrix} = \begin{bmatrix} R_a & 0 & 0 & 0 & 0 \\ 0 & R_b & 0 & 0 & 0 \\ 0 & 0 & R_c & 0 & 0 \\ -\frac{r_a}{i_a} & -\frac{r_b}{i_b} & -\frac{r_c}{i_c} & D & 0 \\ 0 & 0 & 0 & -1 & 0 \end{bmatrix} \begin{bmatrix} i_a \\ i_b \\ i_c \\ \omega \\ \theta \end{bmatrix} + \begin{bmatrix} L_a & 0 & 0 & 0 & i_a \frac{\partial L_a}{\partial \theta} \\ 0 & L_b & 0 & 0 & i_b \frac{\partial L_b}{\partial \theta} \\ 0 & 0 & L_c & 0 & i_c \frac{\partial L_c}{\partial \theta} \\ 0 & 0 & 0 & J & 0 \\ 0 & 0 & 0 & 0 & 1 \end{bmatrix} \begin{bmatrix} \dot{i}_a \\ \dot{i}_b \\ \dot{i}_c \\ \dot{\omega} \\ \dot{\theta} \end{bmatrix} \quad (14)$$

where:

$$r_a = \frac{\partial W_a^{co}}{\partial \theta}; \quad r_b = \frac{\partial W_b^{co}}{\partial \theta}; \quad r_c = \frac{\partial W_c^{co}}{\partial \theta}. \quad (15)$$

The matrix of states in equation (14) completely describes the dynamic behavior of the SRG.

## 6. Conversion methods of Wind energy

The wind is an intermittent and variable energy source both in magnitude and in direction. There are several components in wind speed ( $W_{wind}$ ). The capture of the wind energy, in an efficient way, requires the existence of a constant wind flow sufficiently strong (Henaou & Bassily, 1997).

Currently wind turbines are designed to achieve a maximum power at wind speeds above 10 m/s. However, they can be adjusted to the local wind profile.

The maximum theoretical efficiency for the wind to energy conversion is 59.3% (Betz's Limit). The effective efficiency conversion is given by the Power Coefficient ( $C_p$ ), which is expressed by the following, where  $P_{mec}$  is the mechanical power of the turbine and  $P_w$  is the available wind power.

$$C_p = \frac{P_{mec}}{P_w} \quad (16)$$

The power  $P_w$  is related with the wind speed  $V_w$  calculated by (17),

$$P_w = \frac{1}{2} \rho A V_w^3, \quad (17)$$

where  $\rho$  is the air density ( $\rho = 1.225 \text{ kg/m}^3$ ) and  $A$  is the cross-sectional area of the turbine rotor.

When considering the generator efficiency ( $\eta$ ), the output power is given by (18).

$$P_{out} = \frac{1}{2} \rho A V_w^3 (\eta C_p) \quad (18)$$

The power coefficient  $C_p$  is the fraction of the wind kinetic power that is captured by the wind turbine blades (Lobato & Pires, 2003). It is efficiency of the rotor. This coefficient changes from turbine to turbine and its value is given by (19).

The power coefficient  $C_p$  varies with the Speed Ratio ( $\lambda$ ), given in (20).

$$C_p = 0,22 \rho V_w^3 (\eta C_p), \quad (19)$$

$$\lambda = \frac{r \omega}{V_w}, \quad (20)$$

where:  $r$  is the rotor radius,  $\omega$  is the rotor speed.

The low rotor speeds of the turbine bring about small turbulences in the air flow. With high speeds the turbine behaves as a wall for the wind. Therefore the priority is to adapt the wind speed to the rotor speed with the purpose of obtaining a greater conversion efficiency, which results in a maximum  $C_p$  (Gail & Hansen (2006).

The power coefficient  $C_p$  versus speed ratio, for a generic turbine is shows in Figure 9.

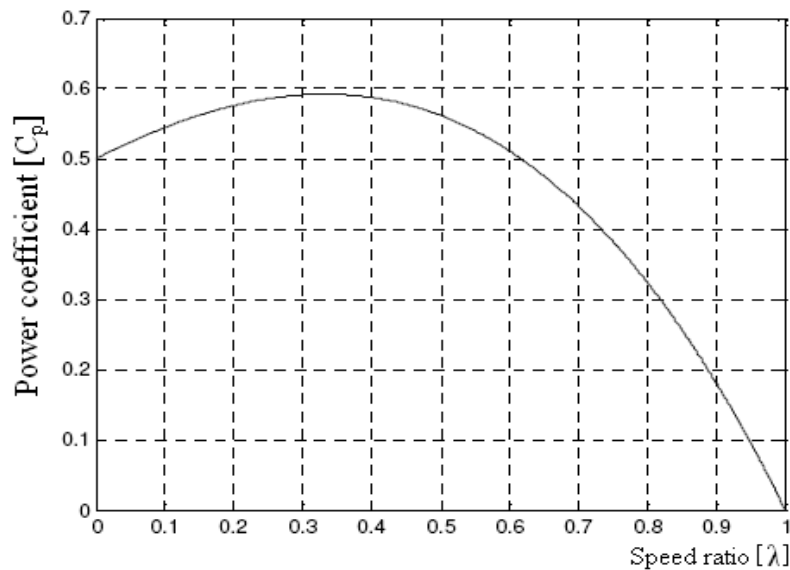


Fig. 9. Power coefficient versus speed ratio for a generic wind turbine.

It can be seen that this coefficient is maxim at around 0.59, then the maximum transfer of energy takes place with almost 60% of the initial value. For turbines of three blades and low speed, the efficiency of the rotor is between 0.2 and 0.4.

It is consensual appreciation that the wind speed in a certain site follows the Weibull probability distribution function like this:

$$p(v_i) = \left(\frac{k}{c}\right) \left(\frac{v_i}{c}\right)^{k-1} e^{-\left(\frac{v_i}{c}\right)^k}, \quad (21)$$

where  $p(v_i)$  is the fraction of time where wind speed  $v_i$  and  $v_i + \Delta v_i$ , divided by  $\Delta v_i$ ,  $c$  is a scale parameter and  $k$  is a shape parameter.

Generally  $p(v_i)$  is expressed in hours per year per m/s. On most places  $c$  varies from 5 to 10 m/s and  $k$  varies between 1.5 and 2.5.

Figure 9 shows the curves of Weibull probability distribution for the shape factor  $k=2$  where the scale parameter varies between 5m/s and 13 m/s.

Figure 10 shows that the wind speed is low most of the time. The rotor speed has the same behavior of the wind speed.

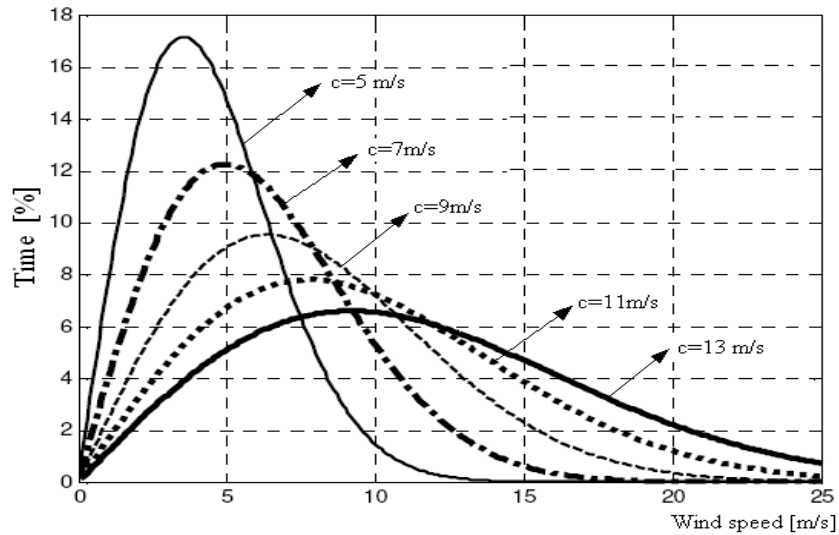


Fig. 10. Wind speed permanency curves.

A generation has to follow this profile should start with low wind speeds and increase of wind speed.

### 7. Wind system simulation

On presents two modes of mechanical coupling of the turbine to the generator: the direct coupling to the turbine shaft, direct - drive wind turbine (Figure 11) and the SRG coupling to the turbine shaft through a gearbox (Figure 13), (Gail & Hansen, 2006).

#### 7.1 Turbine generator direct coupling

The rotor speed  $\omega$  of approximately 100 rad/s is too high and not compatible for this type of wind turbines, in normal wind conditions.

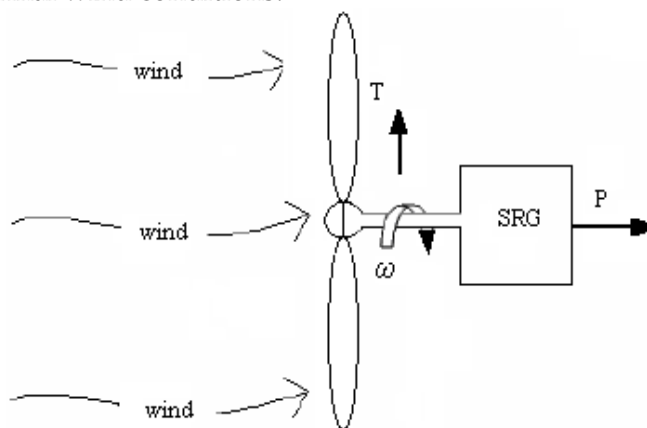


Fig. 11. Direct drive wind turbine with SRG.

Figure 12 shows the electric power generated by the machine coupled with this turbine, where its average power value corresponds to the power of the system excluding losses in the generator.

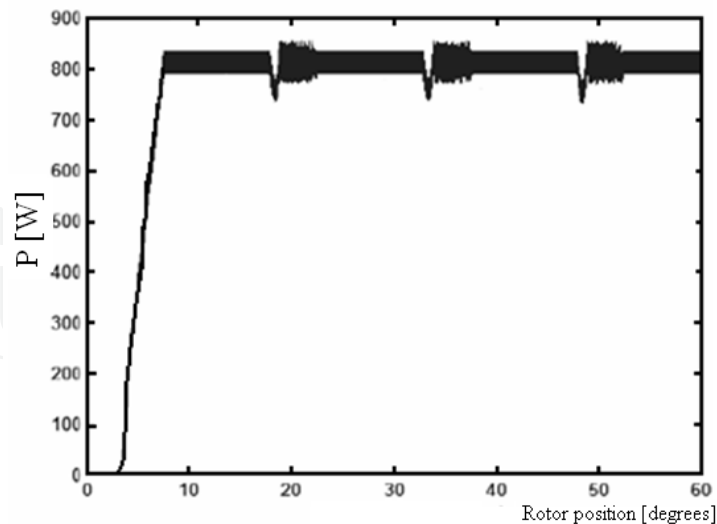


Fig. 12. The 4-phase SRG instantaneous power versus rotor position.

Associated with the required high rotor speed for the good performance of the SRG, the fact that the rotor diameter is small brings about the problem that the wind speed is not sufficient to overcome the combined turbine-generator inertia, namely at the starting stage (Lobato & Pires, 2004).

## 7.2 Indirect coupling with gearbox

Figure 13 indicates the SRG coupling to the turbine shaft through a gearbox.

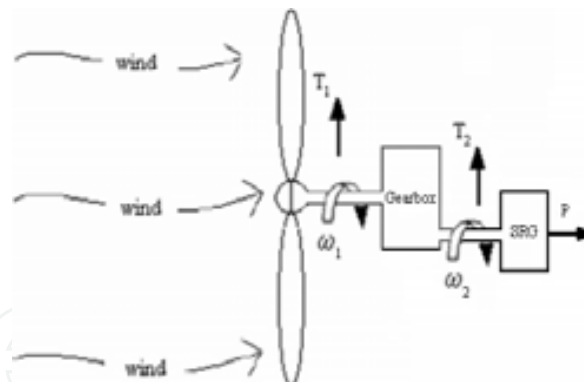


Fig. 13. SRG coupling to the turbine with gearbox.

Assuming that the losses in the gearbox are negligible, and given that the input and output power ( $\omega_1 T_1 = \omega_2 T_2$ ), the transmission ratio  $r_t$ , varies in the inverse of the torque's ratios:

$$r_t = \frac{\omega_1}{\omega_2} = \frac{T_2}{T_1} \quad (22)$$

Figure 14 shows the behavior of the electric power generated by the machine, when coupled with a turbine having a rotor diameter of 5m for a constant wind speed of 8m/s.

With the gearbox the rotor speed of the turbine was reduced to less than half of the value obtained in the first case and the power available in the turbine is close to the rated power in the generator (Lobato & Pires, 2004).

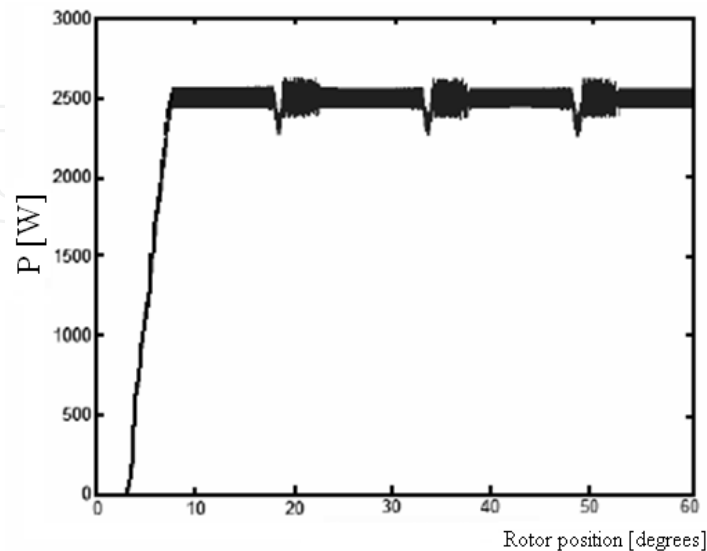


Fig. 14. The 8/6 SRG instantaneous power versus rotor position.

## 8. Conclusion

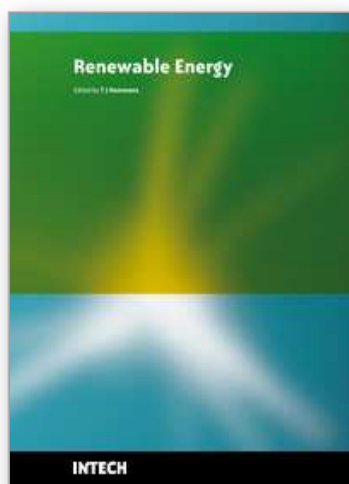
Considering this SRG is a low power machine and therefore produces low torques, it was expectable that too high rotor speeds would develop, which are hardly compatible with the wind speeds typical of this type of energy conversions and with the wind turbines available for these applications (Grauers, 1997).

## 9. References

- Darie El., Cepișcă C., Darie Em. (2009). Advantages of Using a Switched Reluctance Generator (SRG) for Wind Energy Applications, *Proceedings of The International Conference on Ecological Vehicles and Renewable Energies, EVER'09, Monaco, March 26-29, 2009*.
- Darie El., Cepișcă C., Darie Em. (2008). The use of Switched Reluctance Generator in wind applications, *Proceedings of the 13<sup>th</sup> International Power Electronics and Motion Control Conference, EPE-PEMC 2008*, pp. 1986-1989, Poznań, Poland, September 1-3, 2008, ISBN: 978-1-4244-1742-1, IEEE Catalog Number CFP0834A-CDR.
- Darie El., Darie Em., Tcacenco V. (2007) About the permanent magnet Synchronous Machine in wind power applications, *Proceedings of CIEM 2007, 3-rd International Conference on Energy and Environment CIEM 2007*, University Politehnica of Bucharest, November, 22-23 2007.
- Gail G., Hansen A.D. (2006). Controller design and analysis of a variable speed wind turbine with doubly fed induction generator, *Proceedings of the European Wind Energy Conference*, pp. 500-508.



- Lobato P., Pires A. J. (2004). Methodology based on energy-conversion diagrams to optimize switched reluctance generators control, *Proceedings of ICEM 2004*, pp. 700-705.
- Chancharoensook P., Rahman M.F. (2003). Control of a Four-Phase Switched Reluctance Generator: Experimental Investigations, *Proceedings of IEMDC 03*, vol. 2, pp. 842-848.
- Lobato P., Pires A. J. (2003). A New Control Strategy Based on Optimized Smooth-Torque Current Waveforms for Switched reluctance Motors. *Proceedings of Electromotion'03*, vol. 2, 610-615.
- Pan Zai-Ping, Jin Ying, Zhang Hui (2003). Study on switched reluctance generator, *Journal of Zhejiang University*, pp. 594-602, ISSN 1009-3095.
- Torrey D.A. (2002). Switched Reluctance Generator and their control, *IEEE Trans. on Industrial Electronics*, pp. 3-14, Vol. 49, No. 1.
- Zhang H., Pan Z. P. (2003). *Nonlinear inductance mathematical model of Switched Reluctance Generator and its applications*. Proceedings of IEEE International Conference on Small and Medium Electric Machines, pp. 6-9, Vol. 30, No. 3.
- Akhmatov V., Nielsen A. H. (2001). Variable speed wind turbines with multipole synchronous permanent magnet generators, *Proceedings of Wind Engineering*, vol. 27, no. 6, pp. 531-548.
- Chen H., Mang C., Zhao X. (2001). Research on the Switched Reluctance Wind Generator System, Proceedings of IEEE International Conference on Systems, Man and Cybernetics, pp. 1936-1941, Tucson USA.
- Hansen A. D. (2001). Wind models for predictions of power fluctuations from wind farms, *Proceedings of APCWEV*, no.89, pp. 9-18, 2001, Kyoto, Japan.
- Tadashi S. (2001). The switched reluctance generator, *Electronic Control of Switched Reluctance Generator*, *Newness Power Engineering Series*, pp. 227-251, Ed. T. J. E. Miller, Oxford.
- Henao H., Bassily E. (1997). A new control angle strategy for switched reluctance motor, *Proceedings of EPE '97*, vol.3, pp. 613-618, September 1997, Trondheim, Norway.
- Grauers A. (1997). Efficiency of three wind energy generator systems, *IEEE Transactions on Energy Conversion*, vol. 11, no. 3, pp. 650-657.
- Rim G., Krishnan R. (1994). Variable Speed Constant Frequency Power Conversion with A Switched Reluctance Machine, *Proceedings of Applied Power Electronics*, pp. 63-71, APEC'94, Orlando, USA.
- Miller T.J.E., Stephenson J. M., MacMinn, S.R. (1990). Switched Reluctance Drives, *IEEE Tutorial*, IEEE 25 Th IAS Annual Meeting, Seattle, USA.



## **Renewable Energy**

Edited by T J Hammons

ISBN 978-953-7619-52-7

Hard cover, 580 pages

**Publisher** InTech

**Published online** 01, December, 2009

**Published in print edition** December, 2009

Renewable Energy is energy generated from natural resources-such as sunlight, wind, rain, tides and geothermal heat-which are naturally replenished. In 2008, about 18% of global final energy consumption came from renewables, with 13% coming from traditional biomass, such as wood burning. Hydroelectricity was the next largest renewable source, providing 3% (15% of global electricity generation), followed by solar hot water/heating, which contributed with 1.3%. Modern technologies, such as geothermal energy, wind power, solar power, and ocean energy together provided some 0.8% of final energy consumption. The book provides a forum for dissemination and exchange of up-to-date scientific information on theoretical, generic and applied areas of knowledge. The topics deal with new devices and circuits for energy systems, photovoltaic and solar thermal, wind energy systems, tidal and wave energy, fuel cell systems, bio energy and geo-energy, sustainable energy resources and systems, energy storage systems, energy market management and economics, off-grid isolated energy systems, energy in transportation systems, energy resources for portable electronics, intelligent energy power transmission, distribution and inter-connectors, energy efficient utilization, environmental issues, energy harvesting, nanotechnology in energy, policy issues on renewable energy, building design, power electronics in energy conversion, new materials for energy resources, and RF and magnetic field energy devices.

### **How to reference**

In order to correctly reference this scholarly work, feel free to copy and paste the following:

Eleonora Darie, Costin Cepisca and Emanuel Darie (2009). The use of Switched Reluctance Generator in Wind Energy Applications, Renewable Energy, T J Hammons (Ed.), ISBN: 978-953-7619-52-7, InTech, Available from: <http://www.intechopen.com/books/renewable-energy/the-use-of-switched-reluctance-generator-in-wind-energy-applications>

**INTECH**  
open science | open minds

### **InTech Europe**

University Campus STeP Ri  
Slavka Krautzeka 83/A  
51000 Rijeka, Croatia  
Phone: +385 (51) 770 447  
Fax: +385 (51) 686 166  
[www.intechopen.com](http://www.intechopen.com)

### **InTech China**

Unit 405, Office Block, Hotel Equatorial Shanghai  
No.65, Yan An Road (West), Shanghai, 200040, China  
中国上海市延安西路65号上海国际贵都大饭店办公楼405单元  
Phone: +86-21-62489820  
Fax: +86-21-62489821

© 2009 The Author(s). Licensee IntechOpen. This chapter is distributed under the terms of the [Creative Commons Attribution-NonCommercial-ShareAlike-3.0 License](https://creativecommons.org/licenses/by-nc-sa/3.0/), which permits use, distribution and reproduction for non-commercial purposes, provided the original is properly cited and derivative works building on this content are distributed under the same license.

IntechOpen

IntechOpen